# Efficient Compression of Hyperspectral Images Using Optimal Compression Cube and Image Plane

Rui Xiao and Manoranjan Paul

School of Computing and Mathematics
Charles Sturt University, Australia
{rxiao,mpaul}@csu.edu.au

**Abstract.** *Hyperspectral* (HS) images (HSI) provide a vast amount of spatial and spectral information based on the high dimensionality of the pixels in a wide range of wavelengths. A HS image usually requires massive storage capacity, which demands high compression rates to save space with preservation of data integrity. HS image can be deemed as three dimensional data cube where different wavelengths ($W$) form the third dimension along with $X$ and $Y$ dimensions. To get a better compression result, spatial redundancy of HS images can be exploited using different coders along $X$, $Y$, or $W$ direction. This article focuses on taking maximum advantage of HS images redundancy by rearranging HS image into different 3D data cubes and proposes a directionlet based compression scheme constituted the *optimal compression plane* (OCP) for adaptive best approximation of geometric matrix. The OCP, calculated by the spectral correlation, is used to the prediction and determination of which reconstructed plane can reach higher compression rates while minimizing data loss of hyperspectral data. Moreover, we also rearrange the 3D data cube into different 2D image planes and investigate the compression ratio using different coders. The schema can be used for both lossless and lossy compression. Our experimental results show that the new framework optimizes the performance of the compression using a number of coding methods (inclusive of lossless/lossy HEVC, motion JPEG, JPG2K, and JPEG) for HSIs with different visual content.

**Keywords:** Hyperspectral images, lossless compression, and optimal compression plane (OCP).

## 1 Introduction

*Hyperspectral* (HS) images are designed to focus and measure the light reflected by hundreds of narrow and adjacent spectral bands (i.e. wavelengths). HS images may have wide range of wavelengths from hundred nano meter (nm) to thousand micro meter (m) to get different characteristics of objects. The applications of HS imaging are in the fields of military to detect chemical weapon, agriculture to quantify crops, mineralogy to identify different minerals, physics

X. He et al. (Eds.): MMM 2015, Part I, LNCS 8935, pp. 167–179, 2015.

to identify different properties of materials, surveillance to detect different objects and reflections, and environment to measure surface CO2 emissions, to map hydrological formations, and to track pollution levels. A HS camera can capture a HS image with different wavelengths from visual wavelength to far-infrared wavelength. It effectively divides the spectrum into many thin image slices corresponds to wavelength. A commonly used sub-division of wavelengths as follows: *visual* (VIS) from 400 to 700 nano meter (nm), *near infrared* (NIR) from 750 to 1400nm, *shortwave infrared* (SWIR) from 1400 to 3000nm, *medium wave infrared* (MWIR) from 3000 to 8000nm, and *long wave infrared* (LWIR) from 8000 to 15000nm, and *far infrared* from 15000nm to 1000 macro meter (m). Research shows that different materials radiate different reflections in certain range of wavelengths. This characteristic is normally exploited for above mentioned applications. Examples of a HS image and intensity variations in different type objects are shown in Fig. 1 where we can see different slices of a HS image in different wavelength from 400 to 720nm (left) and intensity differences in wavelengths for real and plastic objects.

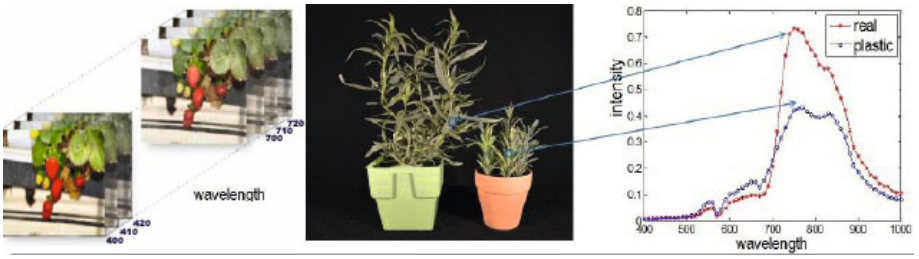


**Fig. 1.** A hyperspectral image (left) with different slices correspond to wavelength and an example of intensities (right) for real and plastic objects in different wavelengths

To illustrate a three-dimensional ( $X, Y, W$) hyperspectral data cube, $X$ and $Y$ represent two spatial dimensions usually deemed as successive natural images, and $W$ represents a range of wavelengths, which is defined as a HS image, $H \in R^{x \times y \times w}$ where R represents the real number values for reflectance of a 3D cube with $X$, $Y$, and $W$ dimensions. The development of these complex image data challenges in the acquisition, transmission and storage. For example, plant phenomics data required processing 1.2TB per day and high-speed hyperspectral camera for monitoring environmental requires 3GB per second [7]. Such volumes already exceed available transmission bandwidths [14]. Efficient compression techniques are therefore needed before HS images can be integrated into the existing and emerging communication systems.

Recent compression methods can fall broadly into two main categories in terms of information preservation: lossless and lossy compression methods [8]. In lossless compression, the original image can be regenerated from the compressed data with small compression ratio; on the other hand, partially distorted image can be generated from the lossy compression methods although

they led higher compression ratios. Some examples of flexible lossy-to-lossless compression techniques are available in the literature [3,4,24]. The compression algorithms based on Discrete Wavelet Transform (DWT) and three dimensional DWT have been presented in [8,20,23]. Huge data blocks are required in these methods that demand a future reduction of the core tensor computations for coding efficiency enhancement and lower the computational load. The compression of multispectral HS image is also considered by using principal component (PC) analysis (PCA) in conjunction with JPEG2000 encoder [3,4,24]. In the PCA-based methods they reduce a number of slices (i.e. 2D images of a certain number of wavelengths) based on the PCA and then apply JPEG2000 on major PCs for efficient rate-distortion performance. Normally, PCA-based compression techniques outperform DWT-based compression techniques for HS images. The reduction of dimensions (i.e., remove some slices) may not be suitable in the compression of HS images because during the PCA it may remove some PCs which are valuable for some specific applications. Some researchers also applied H.264/AVC video coder with the aim of determining its feasibility when applied to HS images compression in [11,18]. They proposed some modifications in the configuration of the coder to exploit different redundancy within HS image for better compression and unmixing applications. So far in our knowledge feasibility analysis of HS image compression using the latest high efficiency video encoder [19] HEVC standard are still deficient in current research.

Recently researchers treat a video as a temporal (along T-axis) collection of two dimensional pictures (formed by $XY$ axes); compress them by exploiting spatial and temporal redundancy in the pictures using different video encoders [9,10,16]. They also define an optimal compression plane (OCP) determination strategy based on the cross-correlation among different directions (i.e., $XYT$, $TXY$, $TYX$) as a preprocessing step to find the best compression plane without applying video coder in each plane exhaustively. The most of the cases the OCP plane can predict the optimal plane which provides the best rate-distortion performance by a coder. In this paper we also treat a HS image as a 3D cube similar to a video as the spectral correlation (band redundancy) is generally high value but not always stronger than spatial correlation [6]. To determine the best 3D cube of a HS image for better compression, we propose an optimal compression cube (OCC) which is the modification of the existing OCP determination strategy [9,10,16]. focusing on the HS image properties in this paper. Then we apply different video and image coding standards such as Motion-JPEG [13,15,22], JPEG [1,12,21], JPG2000 [2,17], and HEVC [16] on the optimal compression cube (OCC) for the best rate-distortion performance. Some compression techniques for example Wavelet transform [5] are not effective in dealing with directional information. Therefore, a directional representation in a 2D dimension $(XY) \times W$, $(YX) \times W$, and $(WX) \times Y$ is also introduced in this paper and investigate the best compression image plane using different image coders. The experimental results show that 2D image plane provides the best rate-distortion performance.

Our contributions in this paper are (i) formulation of an OCC determination strategy based on the HS property, (ii) explore both 3D compression cube and 2D image plane for better compression, (iii) investigate the compressibility of the latest video coding standard HEVC on HS images, and (iv) comprehensive compressibility analysis using different standard image and video coders.

## 2 Proposed Techniques

Finding efficient geometric representations of images is one of the kernel problems to improving HS image compression. The purpose is to reduce the spatial and spectral correlation simultaneously and then archiving or transmitting optimized compression result. We rearrange a HS image into different 3D data cubes and 2D image planes. Subsequently an OCC determination strategy is applied on 3D data cubes to find the best one based on the cross correlation focusing on the HS property. After finding the best 3D data cube plane we apply different image and video coders for actual rate-distortion performance. A HS image can be reconstructed in 6 directions of 3D data cube, $XYW$ (in this direction normally HS images are captured, stored, and display), $YXW$, $WXY$, $XWY$, $WYX$, and $YWX$. Although there are six directions we can form a HS 3D data cube, our experiments using different coders find that two reversed data cubes such as $WXY$ and $XWY$ provide the same rate-distortion performance. Thus, in our experiment we only use three directions (such as $XYW$, $WXY$, and $WYX$) to find the OCC. In addition to 3D formation we also explore directional representation in a 2D dimension $(XY) \times W$, $(YX) \times W$, and $(WX) \times Y$ where two dimensions in bracket form the first dimension and the third dimension forms the second dimension in an image.

The following sub-sections will describe 3D cube formations, 2D image plane formation, OCC formulation, and different encoders used in the proposed technique.

### 2.1 3D Plane Reconstruction

In the sense of data structure of a HS image which contains extensive redundancy among $X$ (i.e. a spatial dimension), $Y$ (i.e. the other spatial dimension), and $W$ (i.e. the wavelenth dimension). Therefore, we need to determine higher redundancy alone different axis before we compress each HS image. In the first step, we aim to construct 3D cube along the different axis of a HS image. Fig. 2 shows a HS image named as *Vase* in different cubic forms. From the figure, we can easily observe that the spatial and spectral correlations in $XYW$, $WXY$ and $WYX$ cubes are different. Thus, a specific coder may exploit the redundancy of a cube better way compared to other coders which justifies the rearrangement of a HS image into different 3D cubes.

### 2.2 2D Plane Reconstruction

As we mentioned earlier some coder may not exploit the directional redundancy in better way, thus we also explore the compressibility of different coders by

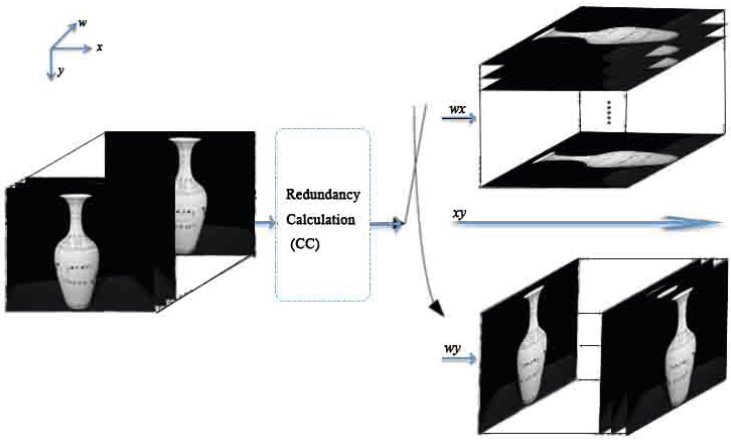


**Fig. 2.** Different 3D data cubes ($XYW$, $WXY$, $WYX$) from where the proposed optimal compression cube algorithm selects the best cube based on the cross correlation, the proposed OCC algorithm and cross correlation equation is defined in Section 2.3

rearranging a HS image into different 2D image planes. Like 3D cube formation, we can make 2D image plane using six directions. Again we find that two reversed image planes have no difference when we apply different image encoders. Three examples of 2D images of the same HS image, Vase are given in Fig. 3 (for better visualization we could not provide whole images in the figure). In our data set, a HS image has 1040139261 resolutions where $X = 1040$, $Y = 1392$, and $W = 61$. We can form 2D images in different directions of a HS image in $X \times (YW)$ i.e., 104084912(=139261), $Y \times (XW)$ i.e., 139263440(=104061), and $W \times (XY)$ i.e., 611447680(=10401392).

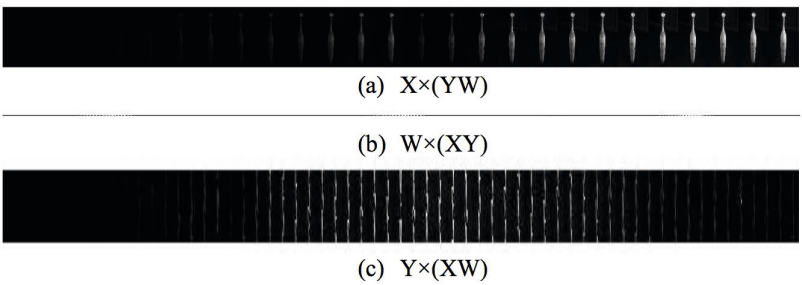


**Fig. 3.** Reconstructed 2D images in different planes

### 2.3 OCC Determination from Different 3D Cubes

Normally when a HS image is captured, slices are organized on a certain wavelength interval. In most cases there are 10 nm. HS images might have two or more bands slices which may or may not be. To obtain value of spatial and spectral redundancies, the average of cross correlation Intra-Band Prediction is used to describe the statistical relationship between neighbouring spectral bands. Then OCC determination will help to choose an optimal cube. The *cross-correlation coefficient* (CC) of *n-th* slice $P_n$ is formulated as follows:

$$CC_n = \frac{\sum_{i,j}((p_n(i,j) - \overline{p_n})(S(i,j) - \overline{S}))}{\sqrt{\sum_{i,j}((p_n(i,j) - \overline{p_n})^2 \sum_{i,j}(S(i,j) - \overline{S})^2}} \quad (1)$$

where $S$ is a median slice of a HIS cube and $P_n$ is the average pixel intensities of *n-th* slice. Unlike the existing OCP scheme [10] we do not calculate the cross correlation coefficient using adjacent slices or frames in the proposed OCC technique. As the property of a HS image is different from the property of a video, we use median slice information to calculate cross correlation coefficient of each slice in different directions. The median slice is the most dominant wavelength of a HS image for major applications and the median slice has the most dominant visual information of a HS image, thus, we use the median slice as the reference slice to calculate CCs. The higher redundancy may reflect in raising the value of CC. We need to determine average CC in each 3D data cube and then the proposed OCC technique find the optimal cube based on the maximum value of average CC from different cubes. The experimental results shown in Fig. 4 reveal that most of the cases $XYW$ cube provides the maximum CC. In the experiment section we also show that the best encoder provides better results in $XYW$ cube in 3D formation in most cases. We also test the rate-distortion performance by different coders based on the predicted direction using the existing OCP technique. The experimental results show that OCP fails to predict the accurate direction for HS images. Thus, this evidence proves the validity of the proposed OCC technique to predict the optimal compression cube direction.

### 2.4 Different Coder and Evaluation Criteria

The performance comparison of OCC is verified using two most popular image compression methods such as Motion JPEG, JPEG and JPEG2000 and the latest video coding standard HEVC. Image coding standards such as JPEG is based on DCT and JPEG2000 and motion JPEG are based on wavelets transformation. For 3D data cube compression we also use the latest video coding standard with limited motion search to exploit the redundancy between adjacent slices or images. To verify compression performance, we use quantitative and qualitative comparison. The quantitative com parison is based on the PSNR (*peak signal to noise ratio*) which is defined as PSNR $=10.log_{10}(MAX_I^2/MSE)$ where $MAX_I$ is the maximum possible pixel value of the image and MSE is the mean square

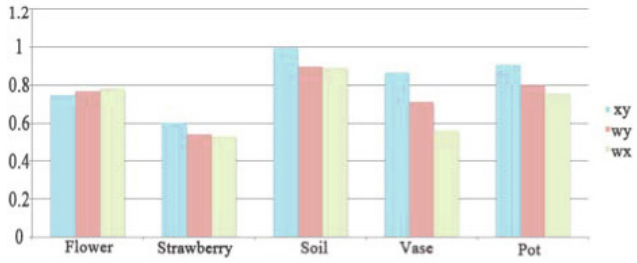


**Fig. 4.** The correlation coefficient along different axes where *xy* axes indicates *XYW* cube, *wy* axes indicates *WYX* cube and *wx* axes indicates *WXY* cube

errors between the original image and the reconstructed image. We also use subjective evaluation by showing reconstructed images using different cube or planes with different encoders.

## 3 Experiments

The proposed algorithms have been applied to different HS images such as *Pot*, *Vase*, *Flower*, *Strawberry*, and *Soil*. In this experiment, we use HEVC video encoder along with image encoders to exploit the redundancy between slices. The quantization parameters (QPs) used in HEVC are from 10 and 51 to see wide range different quality and bit rates where QP=10 provides super quality picture with high bit rates and QP=51 provides inferior quality picture with low bit rates. For all JPEG encoders we use 3 to 93 quantization parameters for a wide range of quality and bit rates where 3 provides lower quality and 93 provides higher quality.

### 3.1 Compression Results Based on 3D Cubes

In this subsection, the OCC framework is validated using image encoders such as JPEG2000, JPEG and HEVC. The PSNR gain is listed based on those coding standards respectively. These examples demonstrate in five HS images: *Pot*, *Soil*, *Vase*, *Flower*, and *Strawberry*.

Fig. 5 shows that the rate-distortion performance in the *XYW* cube is better than the *WXY* or *WYX* cube for all images. This result is also consistence with the proposed OCC strategy where the OCC selects *XYW* cube based on the CC in this direction (see Fig. 4). Although our OCC technique selects different cube as the optimal cube, the best coder provides better rate-distortion performance in *XYW* cube for Flower image. However, the rate-distortion performance of the selected cube by OCC does not perform significant inferior. JPEG2000 with *XYW* cube provides the most distinguishing results compared to other two cubes where *XYW* direction provides comparable results with other coders, however, it provides significantly lower compression results in other two cubes. HEVC does

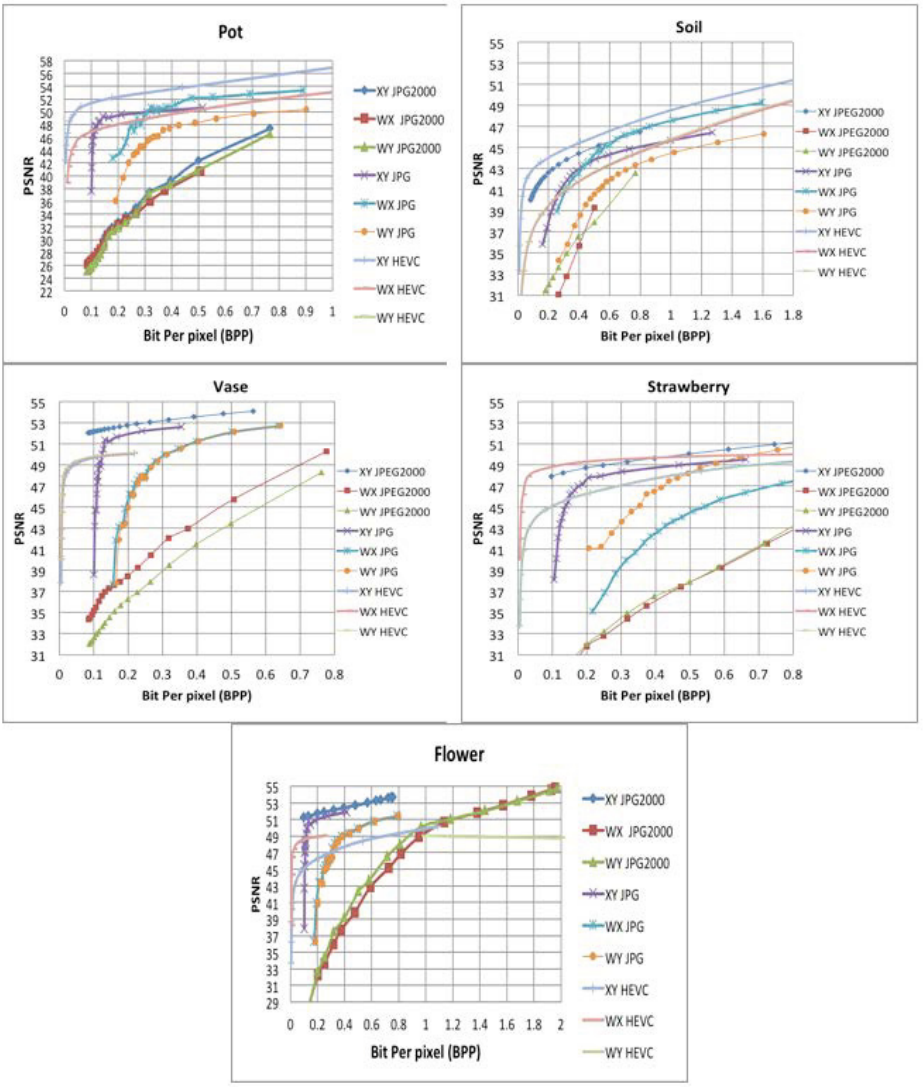


**Fig. 5.** Rate-distortion curves of five standard hyperspectral images using JPEG, JPEG2000, and HEVC coders on three different 3D arrangements (i) $XYW$, (ii) $WXY$, and (iii) $WYX$

**Table 1.** The voting result of the optical compression ratio using HEVC video coder and other image video coders JPEG/JPEG2K

| **Images** | **Low Bit rates 0 to 0.5bpp (+ 35 PSNR or more)** | | | **High bit rate >0.5** | | |
|---|---|---|---|---|---|---|
| Soil | HEVC | JPEG2000 | JPEG | HEVC | JPEG | HEVC |
| | XY | XY | XY | XY | WX | WX |
| Straw- | JPEG2000 | JPEG | HEVC | JPEG2000 | JPEG | JPEG |
| berry | XY | XY | XY | XY | WY | XY |
| Vase | JPEG2000 | JPEG | HEVC | JPEG2000 | JPEG | JPEG |
| | XY | XY | XY | XY | XY | WY |
| Pot | HEVC | JPEG | JPEG | HEVC | JPEG | HEVC |
| | XY | XY | WY | XY | WX | WX |
| Flower | JPEG2000 | JPEG | JPEG | JPEG2000 | JPEG | JPEG |
| | XY | XY | WY | XY | XY | WX |

not provide the best rate-distortion performance compared to the other coders, however, it performs reasonably well with different cubes.

Table. 1 summaries the results shown in Fig. 5 where the coding results of HEVC, JPEG2000 and JPEG are listed and compared among 5 images in terms of PSNR and different bit per pixel (BPP). Table.1 votes the best compression ratio between low bit rates and high bit rates. The experiment demonstrates that HEVC encoder achieves better compression result at $XYW$ and $WXY$ cubes at high bite rate, especially when the BPP is higher than 0.5 or PSNR is more than 35 dB. At low bit rates i.e. below 0.5 BPP and above 35 dB PSNR, $XYW$ cube outperforms mainly. JPEG2000 is also a prime encoder of HSI in both low and higher bit rate.

We also investigate the rate-distortion performance using another popular video compression encoder, Motion JPEG to see the best cube for compression. The experimental results (see show Fig. 6) that Motion JPEG along $XYW$ cube also provides better results compared to other directions.

### 3.2 Compression Results Based on 2D Image Planes

Reconstructed 2D image planes in our experiments demonstrate excellent performance for HS image compression. Corresponding PSNR can reach up to 50 dB at 0.5 BPP. Images well preserve clear edge and patterns information for clear visualization. Rate-distortion curves in Fig. 7 illustrate that the reconstructed image using $X \times (YZ)$ image plane presents noteworthy higher performance comparing to other planes.

In addition to objective result comparison, we also investigate subjective evaluation with the reconstructed images in 2D planes. Fig. 8 demonstrates that reconstructed 2D plane on $Y \times (XW)$ well preserves clear edge and pattern information for better visual perception. Although other two planes $X \times (YW)$

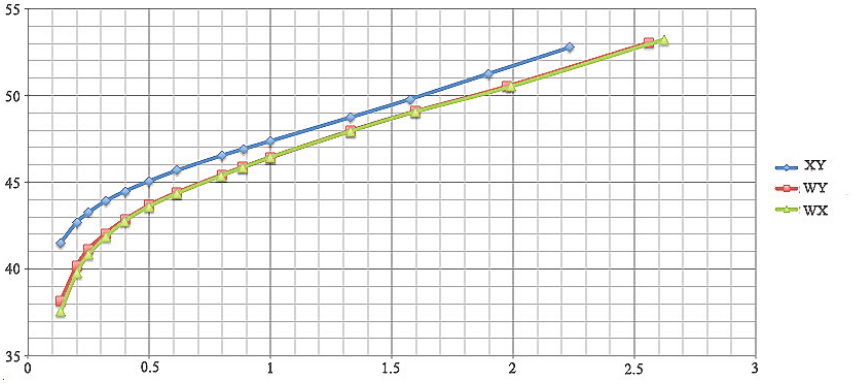


**Fig. 6.** Using Motion JPEG encoder in $XYW$, $WXY$, and $WYX$ cubes for Soil image

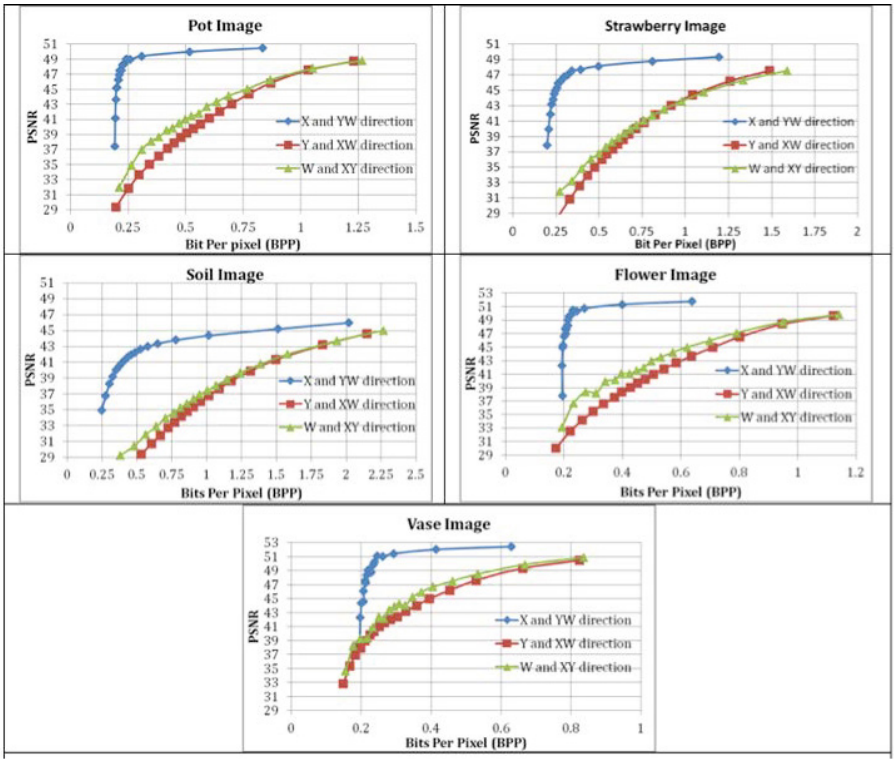


**Fig. 7.** Rate-distortion performance of five standard hyperspectral images using JPEG coder on three different 2D arrangements (i) $X$ and $YW$ i.e., 1040 84912, (ii) $Y$ and $XW$ i.e., 1392 63440, and (iii) $W$ and $XY$ i.e., 611447680

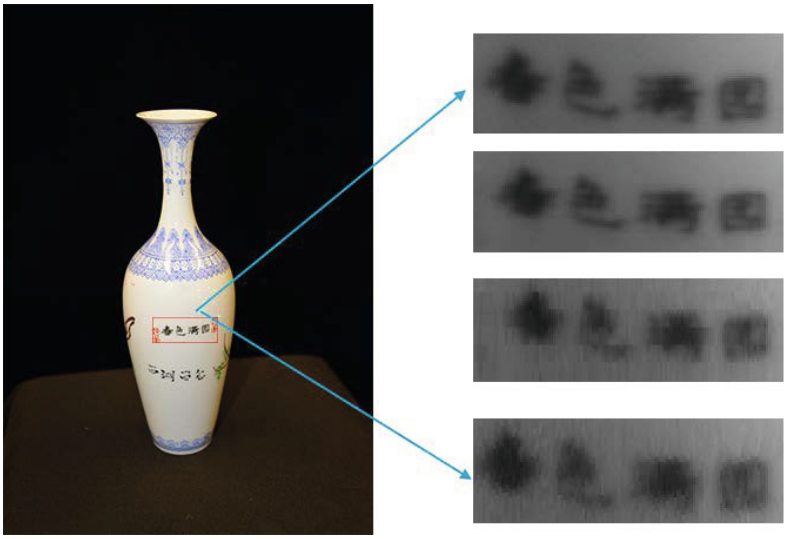

**Fig. 8.** Reconstructed Vase HS image (shows a small part of the Vase image for clear visualization of patterns and edges) for subjective evaluation in different 2D image planes using JPEG encoder; the left sub-figure shows entire slice of Vase HS image, the right sub-figure shows a small part of an original image, reconstructed image using $X \times YW$ plane, $Y \times WX$, and $W \times XY$ from top row to bottom row respectively

and $W \times (XY)$ compressed by same encoding standard in same quality, partial edge information lost can be detected by normal human vision.

## 4 Conclusion

There are a number of methods to compress a hyperspectral images using different transformations and feature extractions strategies. However, in the most of cases they reduce dimensions (i.e., reduce reflectance in some wavelength range) of a hyperspectral image for compression purpose. This may not be appropriate for a number of applications as in this process some valuable information might be removed. In this paper we rearrange a hyperspectral image into different 3D cubes and 2D image planes and then apply popular image and video encoders to see the compression performance by exploiting spatial and spectral redundancy without losing specific wavelength information. To do this we propose an optimal compression cube to predict the optimal 3D cube for the best rate-distortion performance. We confirm that the natural cube (i.e., $XYW$) is the best compression cube. We also confirm that HEVC and JPEG2000 are better encoder where HEVC provides more consistence performance in different directions compared to JPEG2000. Experimental results also show that our proposed optimal compression cube prediction technique can predict the optimal 3D cube successfully in the most cases. The proposed OCC framework is compatible with

any compression encoders and decoders since the required pre-processing is independent of the encoding scheme to be used. The OCC framework is easy to implement with low additional computational complexity, only the simple step of calculation of the CCs need to be involved.

We also investigate the coding performance by rearranging a hyperspectal image into 2D image planes. The experimental results show that an encoder provides the best compression results when we form a 2D plane compared to 3D cube. In future we will test the compressibility of a hyperspectral video.

**Acknowledgments.** We acknowledge that Dr Jun Zhou, Griffith University Australia, provided us datasets and valuable information regarding hyperspectral image processing.

## References

1. Byrne, J., Ierodiaconou, S., Bull, D., Redmill, D., Hill, P.: Unsupervised image compression-by-synthesis within a jpeg framework. In: 15th IEEE International Conference on Image Processing, ICIP 2008, pp. 2892–2895. IEEE (2008)
2. Ciżnicki, M., Kierzynka, M., Kopta, P., Kurowski, K., Gepner, P.: Benchmarking jpeg 2000 implementations on modern cpu and gpu architectures. Journal of Computational Science 5(2), 90–98 (2014)
3. Du, Q., Fowler, J.E.: Hyperspectral image compression using jpeg2000 and principal component analysis. IEEE Geoscience and Remote Sensing Letters 4(2), 201–205 (2007)
4. Du, Q., Ly, N., Fowler, J.E.: An operational approach for hyperspectral image compression. In: 2012 IEEE International Geoscience and Remote Sensing Symposium (IGARSS), pp. 1357–1360 (2012)
5. Gao, X., Lu, W., Tao, D., Li, X.: Image quality assessment based on multiscale geometric analysis. IEEE Transactions on Image Processing 18(7), 1409–1423 (2009)
6. Huo, C., Zhang, R., Peng, T.: Lossless compression of hyperspectral images based on searching optimal multibands for prediction. IEEE Geoscience and Remote Sensing Letters 6(2), 339–343 (2009)
7. Jun, Z.: Hyperspectral imaging in environmental informatics. In: Seminar Presentation at Charles Sturt University (April 16, 2014)
8. Karami, A., Yazdi, M., Mercier, G.: Hyperspectral image compression based on tucker decomposition and wavelet transform. In: 2011 3rd Workshop on Hyperspectral Image and Signal Processing: Evolution in Remote Sensing (WHISPERS), pp. 1–4. IEEE (2011)
9. Liu, A., Lin, W., Zhang, F.: Lossless video compression with optimal compression plane determination. In: IEEE International Conference on Multimedia and Expo, ICME 2009, pp. 173–176. IEEE (2009)
10. Liu, A., Lin, W., Paul, M., Zhang, F., Deng, C.: Optimal compression plane for efficient video coding. IEEE Transactions on Image Processing 20(10), 2788–2799 (2011)
11. Liu, G., Zhao, F., Qu, G.: An efficient compression algorithm for hyperspectral images based on a modified coding framework of h. 264/avc. In: IEEE International Conference on Image Processing, San Antonio, TX, USA, pp. 341–344 (2007)

12. Noor, N.R.M., Vladimirova, T.: Investigation into lossless hyperspectral image compression for satellite remote sensing. International Journal of Remote Sensing 34(14), 5072–5104 (2013)
13. Miaou, S.-G., Ke, F.-S., Chen, S.-C.: A lossless compression method for medical image sequences using jpeg-ls and interframe coding. IEEE Transactions on Information Technology in Biomedicine 13(5), 818–821 (2009)
14. Motta, G., Rizzo, F., Storer, J.A.: Hyperspectral data compression. Springer (2006)
15. Mudassar Raza, A.A., Sharif, M., Haider, S.W.: Lossless compression method for medical image sequences using super-spatial structure prediction and inter-frame coding. J. Appl. Res. Technol. 10(4), 618–628 (2012)
16. Paul, M.: Efficient video coding using optimal compression plane and background modelling. IET Image Processing 6(9), 1311–1318 (2012)
17. Rucker, J.T., Fowler, J.E., Younan, N.H.: Jpeg2000 coding strategies for hyperspectral data. In: Proceedings of the 2005 IEEE International Geoscience and Remote Sensing Symposium, IGARSS 2005, vol. 1, p. 4. IEEE (2005)
18. Santos, L., López, S., Callico, G.M., Lopez, J.F., Sarmiento, R.: Performance evaluation of the h. 264/avc video coding standard for lossy hyperspectral image compression. IEEE Journal of Selected Topics in Applied Earth Observations and Remote Sensing 5(2), 451–461 (2012)
19. Sullivan, G.J., Ohm, J., Han, W.J., Wiegand, T.: Overview of the high efficiency video coding (hevc) standard. IEEE Transactions on Circuits and Systems for Video Technology 22(12), 1649–1668 (2012)
20. Tang, X., Pearlman, W.A., Modestino, J.W.: Hyperspectral image compression using three-dimensional wavelet coding. In: Electronic Imaging 2003, pp. 1037–1047. International Society for Optics and Photonics (2003)
21. Vo, D.T., Nguyen, T.Q.: Quality enhancement for motion jpeg using temporal redundancies. IEEE Transactions on Circuits and Systems for Video Technology 18(5), 609–619 (2008)
22. Wang, Z., Chanda, D., Simon, S., Richter, T.: Memory efficient lossless compression of image sequences with jpeg-ls and temporal prediction. In: Picture Coding Symposium (PCS), pp. 305–308. IEEE (2012)
23. Wu, Y.Q., Wu, C.: Hyperspectral remote sensing image compression based on wavelet and support vector regression. Journal of Astronautics 3, 024 (2011)
24. Zhu, W., Du, Q., Fowler, J.E.: Multitemporal hyperspectral image compression. IEEE Geoscience and Remote Sensing Letters 8(3), 416–420 (2011)